Feshbach spectroscopy of an ultracold ^{41}K-^{6}Li mixture and ^{41}K atoms

Xiang-Pei Liu,[1,2,3] Xing-Can Yao,[1,2,3] Ran Qi,[4] Xiao-Qiong Wang,[1,2,3] Yu-Xuan Wang,[1,2,3] Yu-Ao Chen,[1,2,3] and Jian-Wei Pan[1,2,3]

[1]*Shanghai Branch, National Laboratory for Physical Sciences at Microscale and Department of Modern Physics, University of Science and Technology of China, Shanghai 201315, China*

[2]*CAS Center for Excellence and Synergetic Innovation Center in Quantum Information and Quantum Physics, University of Science and Technology of China, Hefei, Anhui 230026, China*

[3]*CAS-Alibaba Quantum Computing Laboratory, Shanghai 201315, China*

[4]*Department of Physics, Renmin University of China, Beijing 100872, China*

(Received 3 June 2018; published 21 August 2018)

We observe 69 ^{41}K-^{6}Li interspecies Feshbach resonances including 13 elastic p-wave resonances and 6 broad d-wave resonances of ^{41}K atoms in different spin-state combinations at fields up to 600 G. Multichannel quantum-defect theory calculation is performed to assign these resonances and the results show perfect agreement with experimental values after improving input parameters. The observed broad p- and d-wave resonances display a fully resolved multiplet structure. They may serve as important simulators to nonzero partial-wave-dominated physics.

DOI: 10.1103/PhysRevA.98.022704

I. INTRODUCTION

Magnetic Feshbach resonance [1] provides an essential tool in the study of ultracold-atom physics. Several breakthroughs have been demonstrated by tuning the interaction strength with Feshbach resonance, such as the formation of solitons [2,3], the observation of Efimov trimer states [4–6], and the creation of polar molecules [7]. Of particular interest are the broad Feshbach resonances, which are useful for studying universal properties in few-body and many-body atomic systems. Broad s-wave Feshbach resonance offers a great opportunity to study both weak-coupling Bardeen-Cooper-Schrieffer superfluid and Bose-Einstein condensation (BEC) of tightly bound fermion pairs [8–11]. Broad high partial-wave resonances hold great promise for the study of three-body recombination decay [12], the formation of p-wave molecules [13], and the realization of d-wave molecular superfluid [14].

Up to now, Feshbach resonances have been studied in most of the laser-cooled atomic species [1,15,16]. Among them, lithium and potassium atoms have attracted intense interest in both experimental and theoretical studies. Many s- or p-wave resonances have been reported in the isotopes of lithium and potassium [2,17–20], in particular in two broad s-wave resonances in ^{6}Li [21] and ^{40}K [22], respectively. Interspecies Feshbach resonances have been studied in the Fermi-Fermi mixture of ^{6}Li and ^{40}K [23,24]. The potential functions of singlet and triplet states of the lithium-potassium mixture have also been observed [25]. For the Bose-Fermi ^{41}K-^{6}Li mixture, although the superfluid mixture has been realized with the observation of vortex lattices [26], a full description of its Feshbach resonance is still missing. Moreover, the recent observation of a broad d-wave shape resonance in the lowest-energy channel of ^{41}K atoms [14] brings great promise for the investigation of universal physics with strong coupling in nonzero partial waves. Therefore, a more complete search of the d-wave resonances in ^{41}K systems is urgently required.

In this work, we report on an extensive experimental and theoretical study of the s- and p-wave Feshbach resonances in the ^{41}K-^{6}Li mixture and d-wave Feshbach resonances in single-species ^{41}K. We observe 69 interspecies Feshbach resonances in ten spin combinations of the ^{41}K-^{6}Li mixture and six broad d-wave resonances in four spin combinations of ^{41}K atoms (see Fig. 1 for the interested spin channels). We perform semianalytic multichannel quantum-defect theory (MQDT) calculations based on parameters reported in previous literature [25] to identify these resonances. After fine-tuning the singlet and triplet quantum-defect parameters, perfect accord is achieved between the theoretical and experimental results. In the case of interspecies Feshbach resonances, all the observed s-wave resonances are identified as narrow resonances, while several p-wave resonances possess quite wide resonance widths, which are also experimentally ascertained by the distinct doublet structure on the loss spectroscopy. For the single-species ^{41}K system, all the d-wave broad resonances possess a fully resolved triplet structure on the loss spectroscopy, which exactly demonstrates that they are from real d-wave to d-wave coupling [14,27]. Our vast amounts of experimental data and improved scattering parameters are important to the future research on the ^{41}K-^{6}Li mixture and ^{41}K system.

This paper is organized as follows. In Sec. II we briefly introduce the experimental method for preparing the ultracold ^{41}K and ^{6}Li atoms and detecting the scattering resonances therein. In Sec. III the details of the MQDT calculation are given. In Sec. IV we present the results of s-wave and p-wave resonances in the ^{41}K-^{6}Li mixture and d-wave resonances in the single-species ^{41}K system. Section V summarizes and provides an outlook for future work.

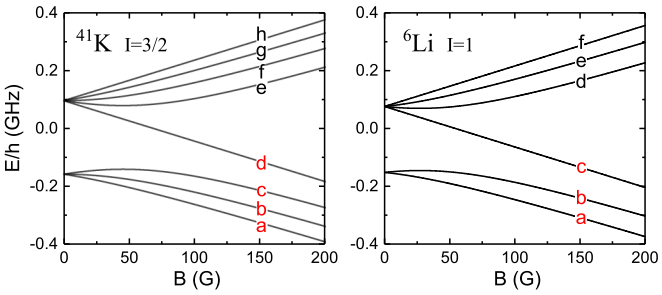

FIG. 1. Magnetic-field dependence of the atomic ground-state energies of ^{41}K and ^{6}Li in different Zeeman levels. The levels of interest are marked in red. Throughout this paper, we use channel $|ab\rangle$ to indicate ^{41}K in $|a\rangle$ and ^{6}Li in $|b\rangle$, or a ^{41}K in $|ab\rangle$ mixture, and so on.

II. EXPERIMENTAL PROCEDURE

The experimental procedure to produce the ultracold ^{41}K-^{6}Li mixture has been described in our previous works [20,26,28]. After radio-frequency (rf) evaporative cooling in the optically plugged magnetic trap, we load about 9×10^6 ^{6}Li and 3×10^6 ^{41}K atoms into a cigar-shaped optical dipole trap and immediately prepare them in the lowest spin states. Then we increase the magnetic field to 435 G and implement an 8-s forced evaporative cooling on ^{41}K atoms by lowering the laser intensity, while the ^{6}Li atoms are sympathetically cooled. Next the cold mixture is adiabatically transferred into a disklike optical dipole trap, where two elliptical laser beams with an aspect ratio of 4:1 are crossed perpendicularly [with a wavelength of 1064 nm, a maximum laser power of each beam of 1.1 W, and a $1/e^2$ axial (radial) radius of 48 μm (200 μm)]. Further evaporative cooling of 8 s is performed within the disklike trap, where the ultracold ^{41}K-^{6}Li mixture with targeted atom numbers and temperatures can be prepared by choosing an appropriate final laser intensity. Finally, absorption imaging along the gravity direction is applied to probe the two species in a single experimental run.

For the s-wave Feshbach resonance measurement, we prepare the mixture at the lowest temperature with 2.2×10^5 ^{41}K atoms at 60 nK or 0.65 the BEC temperature T_c and 5.5×10^5 ^{6}Li atoms at 270 nK or 0.5 the Fermi temperature T_F to reduce the temperature-induced broadened and resonance position shift of the loss spectrum. We mention that the ^{6}Li and ^{41}K atoms cannot reach fully thermal equilibrium because the single spin ^{6}Li atoms can only thermalize through collisions with ^{41}K atoms and the cloud size difference between them is huge. Fortunately, we find this effect does not affect the Feshbach spectroscopy. For the p-wave resonance measurements, to allow atom to tunnel through the centrifugal barrier, we prepare the mixture at higher temperatures with 1.4×10^6 ^{41}K atoms at 350 nK and 1×10^6 ^{6}Li atoms at 480 nK. Next, to prepare different spin-state combinations, several Landau-Zener pulses are successively applied to transfer the ^{6}Li $|a\rangle$ and ^{41}K $|a\rangle$ atoms to the desired spin states with efficiencies higher than 99%.

To facilitate the measurements, we use the same experimental sequence to produce the ultracold ^{41}K atoms, but without loading ^{6}Li atoms at the magneto-optical trap stage. In order to detect the triplet splitting of d-wave resonances, the cloud is prepared at 310 nK, which is slightly below the T_c [14] with more than 1.8×10^6 ^{41}K atoms. Then we fine-tune the rf power of Landau-Zener pulses to prepare the targeted spin combinations of ^{41}K atoms. We mention that the background lifetime for all the spin combinations of the ^{41}K-^{6}Li mixture and pure ^{41}K is more than 10 s, even for the inelastic scattering channels, long enough for the following measurements.

After the initial state preparation, inelastic loss spectroscopy is performed to detect the scattering resonances where enhanced atom losses occur due to three-body decay. For each measurement, to reduce the systematic errors, the magnetic field is ramped from 435 G to a few gauss below or above the resonance in 50 ms, depending on whether the resonance position is below or above 435 G, respectively. Then, after a 100-ms holding time at that magnetic field for equilibrium, the magnetic field is quickly switched to a desired value and holds for some time between 100 ms and 5 s. The waiting time is carefully chosen for different scattering resonances such that an obvious atom loss signal can be acquired and detectable atoms still survive in the trap to reduce the saturation effects. Finally, the magnetic field is ramped back to 435 G to simultaneously detect the remaining ^{6}Li and ^{41}K atom numbers using resonant absorption imaging. It is found that the loss signals of ^{6}Li atoms are not as good as those of ^{41}K atoms, mainly due to the large difference in cloud sizes between the ^{6}Li and ^{41}K clouds. Therefore, we adopt only the results of ^{41}K atoms to derive the parameters of scattering resonances. Moreover, additional measurements on single-species ^{6}Li and ^{41}K atoms are taken to ensure that the observed loss spectra are solely contributed by the interspecies interactions.

III. THEORETICAL PREDICTION OF FESHBACH RESONANCES

To predict the position and other scattering parameters of the Feshbach resonances, we adopt the semianalytical MQDT developed in [29–31]. In this approach, two quantum-defect functions $K_S^c(\epsilon, \ell)$ and $K_T^c(\epsilon, \ell)$ are required as inputs, where ϵ and ℓ are the scattering energy and angular momentum, respectively. When completely neglecting the dependence on ϵ and ℓ and setting $K_S^c(\epsilon, \ell) = K_S^c(0, 0)$ and $K_T^c(\epsilon, \ell) = K_T^c(0, 0)$, we can already obtain most of the resonance positions with reasonable agreement compared to the experimental results [27,32]. However, as pointed out in [32], including the ℓ dependence with a linear form in $K_S^c(\epsilon, \ell)$ and $K_T^c(\epsilon, \ell)$ greatly improves the accuracy and extends the predicting power of this MQDT.

Considering the correction from the ϵ dependence is usually much smaller than that from the ℓ dependence, we choose the following form in the study of ^{41}K-^{6}Li resonances:

$$K_S^c(\epsilon, \ell) = K_S^c(0, 0) + \beta_S \ell(\ell + 1), \tag{1}$$

$$K_S^c(\epsilon, \ell) = K_T^c(0, 0) + \beta_T \ell(\ell + 1). \tag{2}$$

With such a choice of parametrization for $K_S^c(\epsilon, \ell)$ and $K_T^c(\epsilon, \ell)$, all scattering properties in all partial waves and all different hyperfine levels can be determined by four parameters $K_S^c(0, 0)$, $K_T^c(0, 0)$, β_S, and β_T. In turn, these four parameters

can be set with four different known resonance positions in two different ℓ (two resonances for each ℓ) from experiments. In practice, we choose two s-wave resonances at $B = 352.46$ G (channel $|ba\rangle$) and $B = 410.54$ G (channel $|bc\rangle$) and two p-wave resonances at $B = 210.09$ G (channel $|ca\rangle$) and $B = 239.71$ G (channel $|cb\rangle$) to set these four parameters. As a starting point, we first relate the parameters $K^c_{S,T}(0,0)$ to the singlet and triplet scattering lengths a_S and a_T, respectively, through the analytic formula [30,33]

$$\frac{a_{S,T}}{\bar{a}} = \sqrt{2}\frac{K^c_{S,T}(0,0) + \tan(\pi/8)}{K^c_{S,T}(0,0) - \tan(\pi/8)}. \tag{3}$$

If we take $a_S = 42.75a_0$ and $a_T = 60.77a_0$ from the literature [25], we get $K^c_S(0,0) = -3.2704$ and $K^c_T(0,0) = 8.5430$. Taking these values of $K^c_{S,T}(0,0)$ to calculate the s-wave scattering, the predicted resonance positions will deviate from the experimental values from several gauss to dozens of gauss. Fine-tunings of $K^c_{S,T}(0,0)$ are then necessary to get a better fit. Finally, we get $K^c_S(0,0) = -3.1235$ and $K^c_T(0,0) = 8.9785$, which results in the values $a_S = 42.24a_0$ and $a_T = 60.48a_0$. Under these choices, the predicted s-wave resonance positions agree perfectly with experimental results, as shown in Table I.

For the ^{41}K-^{6}Li p-wave resonances, the predicted resonance positions with fine-tuned $K^c_{S,T}(0,0)$ still deviate from the experimental values[1] on the level of 10 G, if we simply neglect the ℓ dependence in $K^c_S(\epsilon,\ell)$ and set $\beta_S = \beta_T = 0$ in Eqs. (1) and (2). Then, by further adjusting the values of $\beta_{S,T}$ to $\beta_S = 0.0455$ and $\beta_T = 0.3407$, we can also get perfect agreement for the p-wave resonances between theory and experimental results, as shown in Table II. As for the ^{41}K resonances, since we focus on the d-wave resonances in this work, we only need two parameters $K^c_S(0,\ell=2)$ and $K^c_T(0,\ell=2)$, which are fixed by two d-wave resonance positions. By choosing the two resonances in the channel $|aa\rangle$ (see Table III), we find $K^c_S(0,\ell=2) = 2.0985$ and $K^c_T(0,\ell=2) = 11.2949$. Similarly, we can also see the excellent quantitative agreement with the experimental data shown in Table III.

Finally, we want to emphasize that, our MQDT approach is supposed to work much better on light alkali-metal atoms while not so good for the heavy ones. The reason for this is twofold: (a) Light atoms usually have smaller hyperfine splitting energy compared to heavy ones, which justifies the neglect of the energy dependence in $K^c_{S,T}(\epsilon,\ell)$, and (b) the effects of anisotropic interactions including magnetic dipole-dipole interaction and second-order spin-orbit coupling are more important in heavy atoms, which are not taken into account in our MQDT calculations. As a result, we expect our MQDT to have a similar predicting power of resonances of light atoms like Li, Na, and K and their mixtures while it may not be so accurate on heavy ones like Rb and Cs.

Besides the resonance position, several other parameters are required for a complete description of a well-isolated

[1]According to the Wigner-Eckart theorem, the resonance positions without dipole-dipole interaction satisfy $(B_0 + 2B_1)/3$ (p wave) and $(B_0 + B_2)/2$ (d wave), respectively, where $B_{0,1,2}$ is the resonance position of $|m| = 0, 1, 2$.

TABLE I. ^{41}K-^{6}Li s-wave Feshbach resonance spectroscopy. Here B_{theor} and Δ_{theor} are the theoretically predicted resonance position and width from the MQDT calculation and B_{expt} and Δ_{expt} are the corresponding experimentally determined values. All the above resonances are identified as narrow resonances. The theoretical widths that are less than 0.01 G are recorded as 0.01 G.

Channel	B_{theor} (G)	Δ_{theor} (G)	B_{expt} (G)	Δ_{expt} (G)
$\|a,a\rangle$	21.15	0.01	21.17(1)	0.13(1)
	31.61	0.32	31.63(1)	0.31(2)
	99.50	0.05	99.56(1)	0.16(1)
	104.04	0.02	104.10(1)	0.14(1)
	335.18	0.96	335.13(1)	0.42(1)
	341.36	0.07	341.29(1)	0.17(2)
$\|b,a\rangle$	34.34	0.01	34.39(1)	0.14(1)
	46.29	0.43	46.33(2)	0.23(3)
	99.30	0.01	99.40(1)	0.14(1)
	114.84	0.05	114.93(1)	0.15(1)
	118.96	0.06	119.04(1)	0.16(1)
	352.46	0.91	352.49(1)	0.72(6)
	361.52	0.33	361.45(1)	0.45(5)
	369.45	0.01	369.20(1)	0.14(1)
$\|c,a\rangle$	35.51	0.01	35.64(6)	0.13(1)
	62.10	0.04	62.14(1)	0.14(1)
	124.29	0.55	124.46(1)	0.26(1)
	128.03	0.05	128.12(1)	0.15(1)
	374.58	0.49	374.52(1)	0.24(1)
	384.14	0.12	384.06(1)	0.16(1)
	393.43	0.42	393.35(1)	0.21(1)
$\|c,b\rangle$	83.83	0.06	83.90(1)	0.15(1)
	154.90	0.04	155.00(1)	0.20(1)
	160.94	0.16	161.04(1)	0.17(1)
	402.20	0.90	402.23(1)	0.36(23)
	409.89	0.17	409.83(3)	0.17(2)
$\|a,b\rangle$	37.57	0.03	37.60(2)	0.69(7)
	49.27	0.06	49.29(8)	3.81(24)
	107.06	0.55	107.21(1)	0.26(1)
	358.90	0.51	358.92(18)	4.68(74)
	367.56	0.14	367.58(4)	1.21(13)
	375.58	0.42	375.55(2)	0.30(3)
$\|a,c\rangle$	78.27	−0.01	78.29(1)	0.26(1)
	88.09	0.02	88.09(1)	1.24(4)
	154.18	0.04	154.29(2)	1.93(10)
	163.95	−0.05	164.04(1)	0.30(3)
	389.38	0.11	389.21(9)	5.26(38)
	398.30	0.32	398.27(5)	2.40(16)
$\|b,b\rangle$	63.86	0.12	63.41(1)	0.21(1)
	130.25	0.23	130.34(2)	0.74(5)
	142.70	−0.02	142.77(1)	0.17(1)
	378.38	0.95	378.37(5)	3.79(15)
	387.58	0.17	387.52(1)	0.65(3)
	396.82	0.30	396.70(1)	0.51(4)
$\|b,c\rangle$	103.98	0.01	104.01(1)	0.52(3)
	172.08	0.01	172.25(8)	0.54(7)
	176.53	0.03	176.64(3)	1.06(1)
	410.54	0.45	410.55(12)	3.92(32)
	417.74	0.12	417.77(7)	1.58(15)
$\|c,c\rangle$	196.11	−0.04	196.21(1)	0.14(1)
	434.16	0.51	434.17(1)	3.13(34)

TABLE I. (*Continued.*)

Channel	B_{theor} (G)	Δ_{theor} (G)	B_{expt} (G)	Δ_{expt} (G)
$\|d, a\rangle$	102.41	0.82	102.44(1)	0.36(2)
	166.75	−0.06	166.86(1)	0.43(2)
	171.33	3.54	171.44(1)	0.48(3)
	402.36	0.14	402.33(2)	0.95(5)
	410.02	0.46	409.94(1)	0.61(3)

resonance. Close to each ℓ-wave resonance, we have

$$a_\ell(B) = a_{bg\ell}\left(1 - \frac{\Delta_B}{B - B_{\text{res}}}\right), \tag{4}$$

where a_ℓ is the generalized ℓ-wave scattering length or the so-called scattering hypervolume and B_{res} is the position of the resonance. Another two parameters ζ_{res} and $\delta\mu$ are defined through the leading-order energy and magnetic-field dependence of the quantum defect $K_\ell^{c0}(\epsilon, B)$ around $\epsilon = 0$ and $B = B_{\text{res}}$ [34],

$$K_\ell^{c0}(\epsilon, B) = -w_\ell \zeta_{\text{res}}^{-1} \frac{\epsilon - \delta\mu\delta B}{E_6} + O(\epsilon^2, \delta B^2, \delta B\epsilon), \tag{5}$$

where $\delta B = B - B_{\text{res}}$, $w_\ell = [(2\ell + 3)(2\ell - 1)]^{-1}$, and $E_6 = \hbar^2/m\beta_6^2 = E_{vdW}/4$.

The quantity ζ_{res} characterizes whether the resonance is open-channel ($|\zeta_{\text{res}}| \gg 1$) or closed-channel ($|\zeta_{\text{res}}| \ll 1$) dominated. It was shown that $\zeta_{\text{res}} > 0$ for the s wave and $\zeta_{\text{res}} < 0$ for all high partial waves [34]. For a Feshbach resonance, $\delta\mu$ defined in Eq. (5) is approximately equal to the magnetic moment difference between the free-atom pair and the closed-channel molecule. However, for a shape resonance, since there is no closed-channel molecule, the value of $\delta\mu$ does not have such a physical meaning. We can also show that $\zeta_{\text{res}}\, a_{bg\ell}$, $\delta\mu$, and Δ_B are related as

$$\zeta_{\text{res}} = -w_\ell \frac{a_{bg\ell}}{\bar{a}_\ell} \frac{\delta\mu\Delta_B}{E_6}. \tag{6}$$

The above resonance parameters provide a complete description for each isolated resonance and are shown in Tables I–III.

IV. EXPERIMENTAL RESULTS

A. *s*-wave Feshbach resonances in the ^{41}K-^{6}Li mixture

We study the ^{41}K-^{6}Li interspecies s-wave Feshbach resonances for ten different spin combinations, including four elastic channels ($|aa\rangle$, $|ba\rangle$, $|ca\rangle$, and $|cb\rangle$) and six inelastic ones ($|ab\rangle$, $|ac\rangle$, $|bb\rangle$, $|bc\rangle$, $|cc\rangle$, and $|da\rangle$). Figure 2 shows a typical inelastic loss spectrum of ^{41}K for channel $|ca\rangle$, which is fitted with the asymmetric Lorentz function $N \propto 1/[4(B - B_0)^2 + \omega^2]$, where $\omega = 2\omega_0/\{1 + \exp[F(B - B_0)]\}$, with F the asymmetry parameter. It is quite interesting that the distance between two neighboring resonances is nearly identical and the resonance width decreases monotonically from the low field to the high field, which we also find for $|ba\rangle$, $|ca\rangle$, $|ab\rangle$, and $|bb\rangle$ channels. For all ten spin combinations, we successfully find 56 s-wave Feshbach resonances for a magnetic-field range between 0 and 600 G, which are summarized in Table I. The magnetic-field accuracy is calibrated by rf spectroscopy between the two lowest hyperfine states of ^{41}K atoms for several magnetic-field values and it is found to be better than 10 mG.

B. *p*-wave Feshbach resonances in the ^{41}K-^{6}Li mixture

The p-wave resonances in the ^{41}K-^{6}Li mixture are measured in the four elastic channels $|aa\rangle$, $|ba\rangle$, $|ca\rangle$, and $|cb\rangle$. Figure 3 shows two typical p-wave Feshbach resonances in the $|cb\rangle$ channel. The unambiguous doublet structure of the loss spectrum gives direct evidence of the p-wave resonance, where the two peaks correspond to $|m| = 0$ and $|m| = 1$ resonances due to the magnetic dipolar interactions [35]. The large doublet splitting often implies that the p-wave resonances are broad, which is also confirmed by the calculated resonance parameter. Moreover, all of the loss curves display an asymmetric shape. This is because the atoms can access the quasibound states that lie above the threshold of the open channel due to their

TABLE II. ^{41}K-^{6}Li p-wave Feshbach resonance spectroscopy. Here B_{theor} and Δ_{theor} are the theoretically predicted resonance position and width from MQDT calculation and B_{expt} and Δ_{expt} are the corresponding experimentally determined values.

Channel	B_{theor} (G)	Δ_{theor} (G)	B_{expt} (G) ($\|m\| = 0$)	Δ_{expt} (G) ($\|m\| = 0$)	B_{expt} (G) ($\|m\| = 1$)	Δ_{expt} (G) ($\|m\| = 1$)	ζ_{res}	$\delta\mu/\mu_B$	$a_{bg}/\bar{a}_l$
$\|a, a\rangle$	154.23	18.89	154.42(1)	0.17(2)	154.19(1)	0.17(1)	−0.40	1.48	2.64
	179.64[a]	0.27	179.64(3)	0.12(5)			−0.002	1.89	0.64
$\|b, a\rangle$	24.66	−18.19	24.26(1)	0.16(1)	24.97(1)	0.17(1)	−0.22	−0.71	3.22
	150.59	20.25	151.01(1)	0.17(1)	150.43(1)	0.17(1)	−0.30	0.82	3.30
	187.57[a]	11.95	187.66(1)	0.13(2)			−0.09	1.37	1.04
$\|c, a\rangle$	25.44[a]	−53.99	25.60(1)	0.17(1)			−0.23	−1.06	0.73
	65.25	−10.25	64.71(1)	0.15(2)	65.68(1)	0.16(1)	−0.13	−0.72	3.38
	168.66	11.23	169.19(1)	0.16(2)	168.50(1)	0.16(1)	−0.14	0.65	3.44
	210.09	−8.52	210.19(1)	0.17(2)	210.06(1)	0.13(3)	−0.14	1.40	2.20
	226.76	6.73	226.91(2)	0.22(9)	226.77(1)	0.15(1)	−0.06	1.74	0.93
$\|c, b\rangle$	74.20	−17.10	73.74(7)	0.15(7)	74.55(4)	0.16(2)	−0.30	−1.07	3.00
	205.40	22.41	205.79(2)	0.15(1)	205.33(1)	0.15(1)	−0.34	0.97	2.92
	239.71	2.37	239.77(39)	0.14(9)	239.72(20)	0.15(11)	−0.02	1.50	0.86

[a]Resonance where we observe only a single loss peak.

TABLE III. ^{41}K d-wave Feshbach resonance spectroscopy. Here B_{theor} and Δ_{theor} are the theoretically predicted resonance position and width from MQDT calculation and B_{expt} and Δ_{expt} are the corresponding experimentally determined values.

Channel	B_{theor} (G)	Δ_{theor} (G)	B_{expt} (G) ($\|m\|=0$)	Δ_{expt} (G) ($\|m\|=0$)	B_{expt} (G) ($\|m\|=1$)	Δ_{expt} (G) ($\|m\|=1$)	B_{expt} (G) ($\|m\|=2$)	Δ_{expt} (G) ($\|m\|=2$)	ζ_{res}	$\delta\mu/\mu_B$	$a_{bg}/\bar{a}_l$
$\|a,a\rangle$	17.79[a]	−184.4	16.83(1)	0.44(2)	17.19(6)	0.28(8)	18.75(1)	0.26(5)	−263	−12.22	9.01
	530.38	4.54	530.48(1)	0.17(3)	530.40(4)	0.13(3)	530.18(2)	0.15(2)	−2.50	1.98	21.47
$\|a,b\rangle$	25.47[a]	1804.3	25.31(2)	0.28(5)	25.41(23)	0.17(40)	25.74(1)	0.43(3)	−258	−10.16	−1.09
	544.15	3.23	544.93(1)	0.16(1)	544.79(1)	0.16(2)	544.34(11)	0.15(15)	−1.76	1.98	21.25
$\|b,b\rangle$	64.79[a]	−999.4	63.30(1)	0.38(4)	63.69(8)	0.30(16)	65.16(6)	0.45(9)	−16.5	−0.58	2.21
	564.11	5.56	565.23(4)	0.17(5)	565.05(1)	0.16(5)	564.53(3)	0.15(6)	−0.43	0.30	20.06
$\|c,c\rangle$	105.66[a]	−185.1	104.47(1)	0.43(5)	104.95(1)	0.32(4)	106.27(1)	0.34(3)	−126	−5.99	8.76

[a]Broad shape resonance (all others are broad Feshbach resonances).

nonzero kinetic energy and thus cause enhanced loss of them. Another intriguing feature is the asymmetric shape inversion of the two loss spectra. In Fig. 3(a), the threshold edge of the two resonances appears on the low-magnetic-field side, while in Fig. 3(b) it appears on the high-magnetic-field side. We attribute this to the different sign of $\delta\mu$. If $\delta\mu > 0$ ($\delta\mu < 0$), the molecular state moves upward (downward) with respect to the threshold of the open channel with increasing magnetic field, which implies that the quasibound states exist at the higher (lower) magnetic field. In addition, the locations of $|m| = 0$ resonances are also inverted due to the different sign of $\delta\mu$, which will be at higher (lower) field for $\delta\mu > 0$ ($\delta\mu < 0$).

The 13 experimentally measured p-wave Feshbach resonances are tabulated in Table II, where ten broad p-wave resonances are identified with a doublet structure. For the three narrow p-wave resonances observed, only one loss peak can be detected, possibly limited by the small splitting and the controlled resolution of our magnetic field.

C. d-wave resonance of ^{41}K atoms

For this study, we are only interested in the broad d-wave resonances. We find six broad d-wave resonances in four spin combinations of ^{41}K atoms ($|aa\rangle$, $|ab\rangle$, $|bb\rangle$, and $|cc\rangle$), as shown in Table III. Together with the one we reported in Ref. [14], four of them are shape resonances, while the other three are Feshbach resonances. As an example, Fig. 4 shows the loss curves of two d-wave resonances in the $|bb\rangle$ channel, where the one at lower magnetic field is a shape resonance. They both display a triplet structure and an asymmetric shape, hallmarks of the d-wave resonance. As for the p-wave resonance, three peaks of the d-wave resonance correspond to $|m| = 0, 1, 2$ resonances, which is also due to magnetic dipolar interactions. Furthermore, the asymmetric shape inversions are also observed due to the different sign of $\delta\mu$ for these two resonances. Note that for the observed d-wave resonance, the loss of the $|m| = 0$ resonance is much larger than the $|m| = 1, 2$ resonances, which is because the dipolar interaction

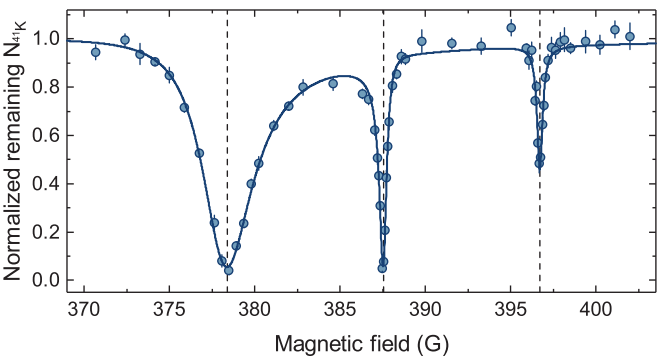

FIG. 2. Normalized remaining atom number of ^{41}K as a function of magnetic field, near three s-wave resonances in the ^{41}K-^{6}Li channel $|ca\rangle$. The solid line is the multipeak asymmetric Lorentz fitting curve. The vertical dashed lines mark the fitted resonance positions. All the data points are averaged out of five records and the error bars represent the standard deviations.

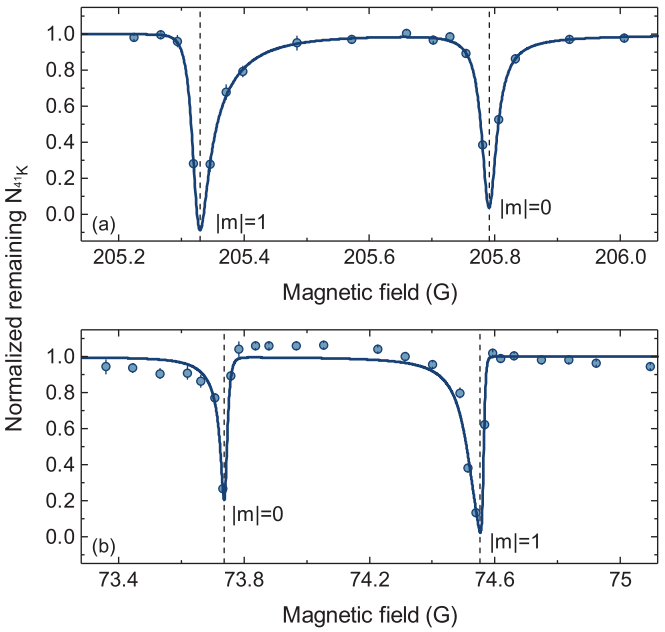

FIG. 3. Normalized remaining atom number of ^{41}K as a function of magnetic field, in the vicinity of two p-wave resonances in channel $|cb\rangle$. The solid lines are the multipeak asymmetric Lorentz fitting curves. The vertical dashed lines mark the fitted resonance positions. We can see an obvious doublet structure in both (a) and (b). Because of the different sign of the $\delta\mu$, the distributions of $|m| = 0$ and $|m| = 1$ resonances are inverted. All the data points are averaged out of five experimental records and the error bars represent the standard deviations.

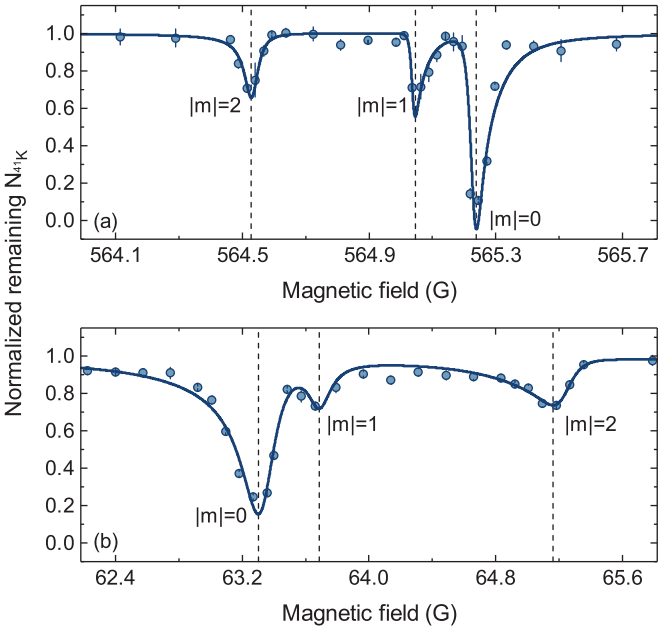

FIG. 4. Normalized remaining atom number of ^{41}K as a function of magnetic field, near two d-wave resonances in channel $|bb\rangle$ of ^{41}K. The solid lines are the multipeak asymmetric Lorentz fitting curves. The vertical dashed lines mark the fitted resonance positions. We can see an obvious triplet structure in both (a) and (b). Because of the different sign of the $\delta\mu$, the distributions of $|m| = 0, 1, 2$ resonances are inverted. All the data points are averaged out of three experimental records and the error bars represent the standard deviations.

can couple the s-wave scattering state to a d-wave bound state with $|m| = 0$, while this is not the case for the p-wave resonance. Moreover, when the ^{41}K atoms are further cooled to form a pure BEC, i.e., without visible thermal atoms, the two peaks associated with $|m| = 1$ and $|m| = 2$ resonances disappear. This is because in such a temperature, the kinetic energy of atoms is too small to penetrate the d-wave centrifugal barrier and thus the atomic loss induced by d-wave scattering is negligible. We mention that all the features described above are observed for all the reported d-wave resonances.

V. CONCLUSION AND OUTLOOK

We have done an intensive experimental study of the Feshbach resonances of the ^{41}K-^{6}Li mixture and d-wave Feshbach resonances of ^{41}K with the aid of MQDT calculations and confirmed the resonance positions with very high accuracy. Several pretty wide p-wave resonances in the ^{41}K-^{6}Li mixture and extremely broad d-wave resonances in the single-species ^{41}K system were discovered. Both p- and d-wave resonances have experimentally resolvable doublet or triplet structures, respectively. The long background lifetime of the states possessing p- or d-wave resonances enables our system to be an ideal platform to pursue many important nonzero partial-wave-related physics.

ACKNOWLEDGMENTS

We are indebted to P. Zhang, H. Zhai, and B. Gao for valuable discussions. This work was supported by NSFC of China (under Grants No. 11874340, No. 11425417 and No. 11774426), the National Key R&D Program of China (under Grants No. 2018YFA0306501 and No. 2018YFA0306502), the CAS, the Anhui Initiative in Quantum Information Technologies and the Fundamental Research Funds for the Central Universities (under Grant No. WK2340000081). R.Q. was supported by the Research Funds of Renmin University of China (under Grants No. 15XNLF18 and No. 16XNLQ03).

[1] C. Chin, R. Grimm, P. Julienne, and E. Tiesinga, Rev. Mod. Phys. **82**, 1225 (2010).
[2] L. Khaykovich, F. Schreck, G. Ferrari, T. Bourdel, J. Cubizolles, L. D. Carr, Y. Castin, and C. Salomon, Science **296**, 1290 (2002).
[3] K. E. Strecker, G. B. Partridge, A. G. Truscott, and R. G. Hulet, Nature (London) **417**, 150 (2002).
[4] T. Kraemer, M. Mark, P. Waldburger, J. G. Danzl, C. Chin, B. Engeser, A. D. Lange, K. Pilch, A. Jaakkola, H.-C. Nägerl, and R. Grimm, Nature (London) **440**, 315 (2006).
[5] M. Zaccanti, B. Deissler, C. D'Errico, M. Fattori, M. Jona-Lasinio, S. Müller, G. Roati, M. Inguscio, and G. Modugno, Nat. Phys. **5**, 586 (2009).
[6] S. Knoop, F. Ferlaino, M. Mark, M. Berninger, H. Schöbel, H.-C. Nägerl, and R. Grimm, Nat. Phys. **5**, 227 (2009).
[7] K.-K. Ni, S. Ospelkaus, M. H. G. de Miranda, A. Pe'er, B. Neyenhuis, J. J. Zirbel, S. Kotochigova, P. S. Julienne, D. S. Jin, and J. Ye, Science **322**, 231 (2008).
[8] C. A. Regal, M. Greiner, and D. S. Jin, Phys. Rev. Lett. **92**, 040403 (2004).
[9] T. Bourdel, L. Khaykovich, J. Cubizolles, J. Zhang, F. Chevy, M. Teichmann, L. Tarruell, S. J. J. M. F. Kokkelmans, and C. Salomon, Phys. Rev. Lett. **93**, 050401 (2004).
[10] C. Chin, M. Bartenstein, A. Altmeyer, S. Riedl, S. Jochim, J. H. Denschlag, and R. Grimm, Science **305**, 1128 (2004).
[11] M. W. Zwierlein, J. R. Abo-Shaeer, A. Schirotzek, C. H. Schunck, and W. Ketterle, Nature (London) **435**, 1047 (2005).
[12] H. Suno, B. D. Esry, and C. H. Greene, New J. Phys. **5**, 53 (2003).
[13] J. P. Gaebler, J. T. Stewart, J. L. Bohn, and D. S. Jin, Phys. Rev. Lett. **98**, 200403 (2007).
[14] X.-C. Yao, R. Qi, X.-P. Liu, X.-Q. Wang, Y.-X. Wang, Y.-P. Wu, H.-Z. Chen, P. Zhang, H. Zhai, Y.-A. Chen, and J.-W. Pan, arXiv:1711.06622v1.
[15] A. Frisch, M. Mark, K. Aikawa, F. Ferlaino, J. L. Bohn, C. Makrides, A. Petrov, and S. Kotochigova, Nature (London) **507**, 475 (2014).
[16] T. Maier, I. Ferrier-Barbut, H. Kadau, M. Schmitt, M. Wenzel, C. Wink, T. Pfau, K. Jachymski, and P. S. Julienne, Phys. Rev. A **92**, 060702 (2015).
[17] S. Jochim, M. Bartenstein, G. Hendl, J. H. Denschlag, R. Grimm, A. Mosk, and M. Weidemüller, Phys. Rev. Lett. **89**, 273202 (2002).
[18] C. D'Errico, M. Zaccanti, M. Fattori, G. Roati, M. Inguscio, G. Modugno, and A. Simoni, New J. Phys. **9**, 223 (2007).

[19] T. Loftus, C. A. Regal, C. Ticknor, J. L. Bohn, and D. S. Jin, Phys. Rev. Lett. **88**, 173201 (2002).
[20] H.-Z. Chen, X.-C. Yao, Y.-P. Wu, X.-P. Liu, X.-Q. Wang, Y.-X. Wang, Y.-A. Chen, and J.-W. Pan, Phys. Rev. A **94**, 033408 (2016).
[21] S. Jochim, M. Bartenstein, A. Altmeyer, G. Hendl, S. Riedl, C. Chin, J. H. Denschlag, and R. Grimm, Science **302**, 2101 (2003).
[22] M. Greiner, C. A. Regal, and D. S. Jin, Nature (London) **426**, 537 (2003).
[23] E. Wille, F. M. Spiegelhalder, G. Kerner, D. Naik, A. Trenkwalder, G. Hendl, F. Schreck, R. Grimm, T. G. Tiecke, J. T. M. Walraven, S. J. J. M. F. Kokkelmans, E. Tiesinga, and P. S. Julienne, Phys. Rev. Lett. **100**, 053201 (2008).
[24] T. G. Tiecke, M. R. Goosen, A. Ludewig, S. D. Gensemer, S. Kraft, S. J. J. M. F. Kokkelmans, and J. T. M. Walraven, Phys. Rev. Lett. **104**, 053202 (2010).
[25] E. Tiemann, H. Knöckel, P. Kowalczyk, W. Jastrzebski, A. Pashov, H. Salami, and A. J. Ross, Phys. Rev. A **79**, 042716 (2009).
[26] X.-C. Yao, H.-Z. Chen, Y.-P. Wu, X.-P. Liu, X.-Q. Wang, X. Jiang, Y. Deng, Y.-A. Chen, and J.-W. Pan, Phys. Rev. Lett. **117**, 145301 (2016).
[27] Y. Cui, C. Shen, M. Deng, S. Dong, C. Chen, R. Lü, B. Gao, M. K. Tey, and L. You, Phys. Rev. Lett. **119**, 203402 (2017).
[28] Y.-P. Wu, X.-C. Yao, H.-Z. Chen, X.-P. Liu, X.-Q. Wang, Y.-A. Chen, and J.-W. Pan, J. Phys. B **50**, 094001 (2017).
[29] B. Gao, Phys. Rev. A **58**, 1728 (1998).
[30] B. Gao, E. Tiesinga, C. J. Williams, and P. S. Julienne, Phys. Rev. A **72**, 042719 (2005).
[31] B. Gao, Phys. Rev. A **78**, 012702 (2008).
[32] C. Makrides and B. Gao, Phys. Rev. A **89**, 062718 (2014).
[33] T. M. Hanna, E. Tiesinga, and P. S. Julienne, Phys. Rev. A **79**, 040701 (2009).
[34] B. Gao, Phys. Rev. A **84**, 022706 (2011).
[35] C. Ticknor, C. A. Regal, D. S. Jin, and J. L. Bohn, Phys. Rev. A **69**, 042712 (2004).